Original Article

Molecular subtype and prognostic model of laryngeal squamous cell carcinoma based on neutrophil extracellular trap-related genes

Guiqin Wu[1], Riqun Jin[1], Jiahua Liao[2], Jianhua Zhang[3], Xuemei Liu[1]

[1]Otorhinolaryngology, Head and Neck Surgery Department, The First Affiliated Hospital of Gannan Medical University, Ganzhou, China; [2]Medical Oncology Department, The First Affiliated Hospital of Gannan Medical University, Ganzhou, China; [3]Academic Affairs Department, The First Affiliated Hospital of Gannan Medical College, Ganzhou, China

Contributions: (I) Conception and design: G Wu; (II) Administrative support: None; (III) Provision of study materials or patients: None; (IV) Collection and assembly of data: G Wu, R Jin, J Liao; (V) Data analysis and interpretation: G Wu, J Zhang, X Liu; (VI) Manuscript writing: All authors; (VII) Final approval of manuscript: All authors.

Correspondence to: Xuemei Liu, MM. Otorhinolaryngology, Head and Neck Surgery Department, The First Affiliated Hospital of Gannan Medical University, No. 23 Youth Road, Ganzhou 341000, China. Email: gnykdyfyliuxuemei@163.com.

Background: Laryngeal squamous cell carcinoma (LSCC) is a prevalent type of head and neck cancer with a poor prognosis due to late diagnosis and limited biomarkers. Neutrophil extracellular traps (NETs) play a critical role in cancer biology, but their involvement in LSCC is not well understood. This study aimed to explore NET's role in LSCC.

Methods: Differentially expressed NET-related genes (DE-NRGs) were identified using GSE10935 datasets and data from The Cancer Genome Atlas (TCGA) database. Functional enrichment and pathway analyses were conducted to elucidate their roles. Consensus clustering identified LSCC molecular subtypes. Immune landscape analyses revealed the tumor microenvironment of different subtypes. A prognostic model was developed using least absolute shrinkage and selection operator (LASSO) regression and validated in external datasets.

Results: We identified 27 DE-NRGs in LSCC, and these genes were involved in heparin binding, cytokine activity, and leukocyte migration. Three molecular subtypes (C1, C2, and C3) were identified, with C3 showing the worst prognosis. Immune landscape analysis revealed significant differences in immune cell infiltration among subtypes. Higher expression of immune checkpoint genes in C2 suggested better immunotherapy outcomes. The prognostic model, based on seven hub DE-NRGs (*ENO1*, *CD44*, *PTX3*, *P2RY14*, *CCL5*, *KLF2*, *MYH9*), demonstrated good predictive performance with area under curve (AUC) values >0.61 for 1-, 3-, and 5-year overall survival. External validation confirmed the model's robustness.

Conclusions: The study identified DE-NRGs as potential biomarkers and developed a robust prognostic model for LSCC. These findings offer insights into LSCC's molecular basis and highlight NETs' role in prognosis and immune landscape.

Keywords: Laryngeal squamous cell carcinoma (LSCC); neutrophil extracellular traps (NETs); prognostic model; immune landscape; molecular subtypes

Submitted Aug 28, 2024. Accepted for publication Jan 18, 2025. Published online Mar 14, 2025.
doi: 10.21037/tcr-24-1531
View this article at: https://dx.doi.org/10.21037/tcr-24-1531

Introduction

Laryngeal squamous cell carcinoma (LSCC) is one of the most common types of head and neck squamous cell carcinoma (HNSC), accounting for approximately 95% of malignant tumors of the larynx and hypopharynx (1). The 5-year overall survival (OS) for patients with advanced LSCC is about 60% (2). Statistically, LSCC affects over 1.7 million people annually, with approximately 123,000 deaths in 2019 attributed to LSCC (3). LSCC is caused by the uncontrolled proliferation of squamous cells on the laryngeal epithelium surface, making delayed diagnosis closely related to poor prognosis. However, due to the insidious onset of early LSCC, the lack of specific symptoms, or asymptomatic nature, it is difficult to detect through routine imaging examinations, which adversely affects the selection of appropriate treatment strategies and clinical outcomes for patients (4,5). To overcome this limitation, discovering new candidate biomarkers is crucial for defining the molecular subtypes of LSCC and constructing prognostic models to guide clinical intervention strategies.

Neutrophils are the most abundant white blood cells in peripheral blood and play roles in anti-inflammation and anti-infection (6). They often respond to microenvironmental factors released by tumors and stromal cells, participating in tumorigenesis and tumor progression (7). Recent studies have emphasized the critical role of the tumor microenvironment (TME) in cancer progression and therapeutic response. In this context, neutrophil extracellular traps (NETs) have emerged as key players in tumor biology. NETs are web-like structures composed of DNA, histones, and granular proteins released by activated neutrophils (8). Traditionally, they are known for capturing and killing pathogens; however, accumulating evidence suggests that NETs can also promote cancer cell proliferation, metastasis, and immune evasion. NETs play multiple roles in cancer-related inflammation, such as promoting tumor growth and distant metastasis (9). Reports have indicated that circulating NET levels are elevated in advanced gastric cancer patients compared to those with localized cancer and healthy individuals (10); NET elimination has been suggested to slow the progression of liver cancer (11); another study found that NET formation can trigger pro-tumor inflammation and promote HCC metastasis (12); NETs can protect cancer cells from immune system attacks, reducing the efficacy of immunotherapy (13). Therefore, NET-related genes (NRGs) have garnered attention as potential biomarkers and therapeutic targets in various cancers. However, studies on NETs in LSCC are rarely reported.

In this study, multiple common databases were utilized to identify molecular subtypes of LSCC based on NRG expression profiles. We constructed a prognostic model composed of NETs using least absolute shrinkage and selection operator (LASSO) Cox regression analysis. This study aimed to elucidate the molecular basis of LSCC and its impact on patient prognosis. The model can provide a valuable tool for risk stratification and personalized treatment planning for LSCC patients. We present this article in accordance with the TRIPOD reporting checklist (available at https://tcr.amegroups.com/article/view/10.21037/tcr-24-1531/rc).

Highlight box

Key findings

- Three distinct molecular subtypes of laryngeal squamous cell carcinoma (LSCC) were identified based on the expression of neutrophil extracellular trap (NET)-related genes (NRGs), and a seven-gene prognostic model related to NETs was constructed.

What is known, and what is new?

- It is known that NETs play a critical role in cancer biology, including tumor growth, metastasis, and immune evasion.
- This study revealed the prognostic significance of NRGs in LSCC and identified seven key NRGs associated with immune-related signaling pathways and patient survival.

What is the implication, and what should change now?

- The identification of distinct molecular subtypes based on NRGs expression may lead to more tailored therapeutic approaches, considering the differential immune landscape and prognosis among subtypes.

Methods

Data acquisition

The study was conducted in accordance with the Declaration of Helsinki (as revised in 2013). The expression profile datasets of LSCC patients GSE10935 (including 12 tumor samples and 12 normal samples) and GSE27020 (including 109 tumor samples and clinical information of patients) were downloaded from the Genomics Expression Omnibus (GEO) database (https://www.ncbi.nlm.nih.gov/geo). The probes in the GEO datasets were changed to corresponding gene names using R package "idmap3"

(https://github.com/jmzeng1314/idmap3). Additionally, the transcriptome and clinical data of LSCC patients were obtained from The Cancer Genome Atlas (TCGA)-NHSC database (https://www.cancer.gov/). After deleting samples without survival time and expression levels, 565 samples were finally enrolled.

NRGs were screened from previous literature (14) and the GeneCards database (https://www.genecards.org) using the keywords "Neutrophil extracellular traps" or "NETosis". After merging and removing duplicate genes, 301 NRGs were finally acquired.

Identification of differentially expressed NRGs (DE-NRGs) in LSCC

Differentially expressed analysis was performed on the GSE10935 and TCGA cohorts to identify differentially expressed genes (DEGs) between normal and tumor samples using R package "limma". The criteria were set as P<0.05 and |log2 fold change| <0.5. Subsequently, the intersecting genes (DE-NRGs) between DEGs and NRGs were screened through a Venn diagram drawn using "VennDiagram". Using R package "clusterProfiler", Gene Ontology (GO) and Kyoto Encyclopedia of Genes and Genomes (KEGG) enrichment analyses were performed on the DE-NRGs, with P<0.05.

Consensus clustering analysis

To further probe into the heterogeneity of LSCC, consensus clustering analysis was conducted on the TCGA cohort using "ConsensusClusterPlus" package in R according to the expression of DE-NRGs. At the same time, the R package "ropls" was used to perform principal components analysis (PCA) dimensionality reduction analysis on the clustering results to compare the heterogeneity among different subtypes.

Immune landscape analysis

The immune cell infiltration analysis was applied to evaluate immune cell abundance in the TCGA cohort through the R package "CIBERSORT" (https://github.com/Moonerss/CIBERSORT). Immune cell infiltration differences and the expression differences of immune checkpoints in different subtypes were compared.

Gene set variate analysis (GSVA)

The background gene set "h.all.v2023.2.Hs.symbols.gmt" was downloaded from the Molecular Signatures Database (MSigDB) (http://www.gsea-msigdb.org/gsea/msigdb). Single sample gene set enrichment analysis (ssGSEA) was then performed on the TCGA cohort to predict pathway scores of each sample using "GSVA" package in R. The differences in pathway scores between different subtypes were compared.

Construction and evaluation of NET-related prognostic model

LASSO Cox regression analysis was then performed on the DE-NRGs using R package "glmnet" to identify hub prognostic DE-NRGs and develop a prognostic model in the TCGA training set (70% of samples, n=399). The regression coefficients and expression levels of hub DE-NRGs were interconnected to calculate the risk score of each sample:

$$\text{Risk score} = \sum_{i=1}^{n} coef_i \times \exp_i \quad [1]$$

All samples were divided into high-risk or low-risk groups according to the median value of risk scores. The prognostic performance was further evaluated in the TCGA testing set (30% of samples, n=166) through Kaplan-Meier (KM) survival analysis and receiver operator characteristic (ROC) curve. An external dataset (GSE27020) was used to validate the robustness of the prognostic model. The model's applicability across different prognostic factors, including age, pathological grade, radiotherapy, targeted therapy, smoking, and alcohol consumption, was further verified.

Statistical analysis

All analyses were performed using R version 4.2.2, and P<0.05 was considered significantly different.

Results

Identification of DE-NRGs in LSCC

There were 1,247 and 7,670 DEGs in the GSE10935

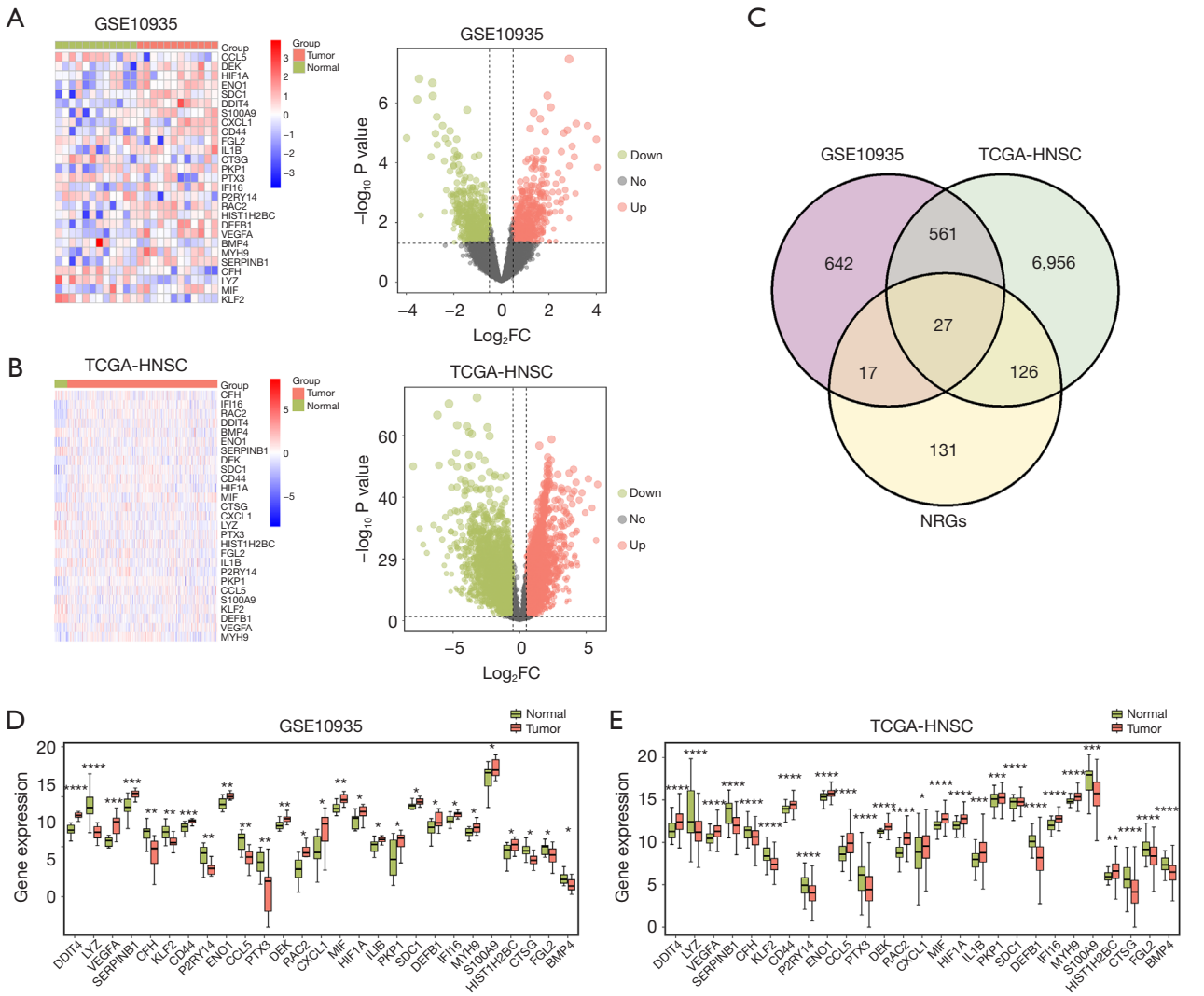

Figure 1 Identification of DE-NRGs in LSCC. (A,B) Heatmap and volcano plot of DEGs between tumor and normal tissues in GSE10935 (A) and TCGA-HNSC cohorts (B). (C) Overlapping genes of DEGs in GSE10935, DEGs in TCGA-HNSC, and NRGs. (D,E) Expression of DE-NRGs in tumor and normal tissues. *, P<0.05; **, P<0.01; ***, P<0.001; ****, P<0.0001. DE, differentially expressed; DEGs, differentially expressed genes; FC, fold change; HNSC, head and neck squamous cell carcinoma; LSCC, laryngeal squamous cell carcinoma; NRGs, neutrophil extracellular trap-related genes; TCGA, The Cancer Genome Atlas.

(*Figure 1A*) and TCGA-HNSC (*Figure 1B*), respectively. The top 27 DEGs were visualized in the heatmap (*Figure 1A,1B*). After intersecting these DEGs and NRGs, 27 DE-NRGs were acquired and shown in the Venn diagram (*Figure 1C*). Gene expression levels of the 27 DE-NRGs in tumor and normal tissues were then analyzed based on the GSE10935 and TCGA-HNSC cohorts. Results revealed significantly different expressions of these genes between tumor and normal tissues in these two cohorts (P<0.05, *Figure 1D,1E*).

Functions of DE-NRGs

Functional enrichment analyses were performed on the DE-NRGs to identify their roles in LSCC. The top five molecular functions were heparin binding, glycosaminoglycan binding, cytokine receptor binding, cytokine activity, and chemoattractant activity (*Figure 2A*).

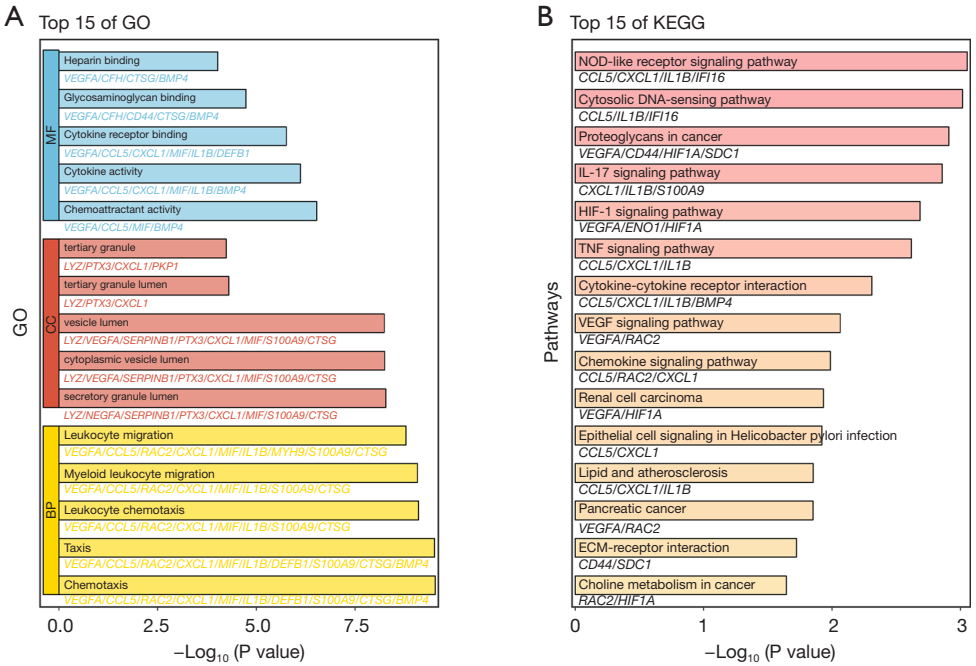

Figure 2 Functions of DE-NRGs. (A) GO enrichment analysis of DE-NRGs. (B) KEGG pathways related to DE-NRGs. BP, biological process; CC, cellular component; DE, differentially expressed; GO, Gene Ontology; KEGG, Kyoto Encyclopedia of Genes and Genomes; MF, molecular function; NRGs, neutrophil extracellular trap-related genes.

Cellular component terms were mainly associated with tertiary granule, tertiary granule lumen, vesicle lumen, cytoplasmic vesicle lumen, and secretory granule lumen (*Figure 2A*). Biological processes were majorly correlated with leukocyte migration, myeloid leukocyte migration, leukocyte chemotaxis, taxis, and chemotaxis (*Figure 2A*). Additionally, DE-NRG-related pathways were mainly enriched in NOD-like receptor signaling pathway, cytosolic DNA-sensing pathway, proteoglycans in cancer, interleukin (IL)-17 signaling pathway, and HIF-1 signaling pathways (*Figure 2B*).

Identification of NET-related molecular subtypes in LSCC

To identify different molecular subtypes of LSCC patients, consensus clustering analysis was conducted on the gene expression profile of 27 DE-NRGs in the TCGA-HNSC cohort. Based on the consensus matrix and cumulative distribution function, k =3 was the optimal number of clusters (*Figure 3A*). Consequently, LSCC patients were classified into three subtypes: C1, C2, and C3 (*Figure 3B*). PCA dimensionality reduction results showed heterogeneity among these three subtypes (*Figure 3C*). Additionally, the KM curve indicated significant differences in survival probability among the three subtypes, with C3 having the worst prognosis (P<0.0001, *Figure 3D*). We further compared the expression of 27 DE-NRGs among these three subtypes. Except for *IFI16* and *DEK*, the other 25 DE-NRGs were significantly differentially expressed among the three subtypes (P<0.001, *Figure 3E*).

Immune landscape in three subtypes

The heterogeneity among different tumor subtypes was related to the TME. Further analyses were performed to analyze the heterogeneity of TME among 3 subtypes. First, GSVA enrichment analysis was conducted to explore NET-related biological characteristics. The enriched pathways are shown in *Figure 4A*, with the top three being the p53 pathway, peroxisome, and glycolysis. GSVA scores of these three pathways were lower in C2 than in C1 and C3 (P<0.05, *Figure 4B*), suggesting potential inhibition of these pathways in C2.

Additionally, immune cell infiltration analysis results indicated that the infiltration levels of B cells, T cells, macrophages M2, dendritic cells, mast cells, and neutrophils

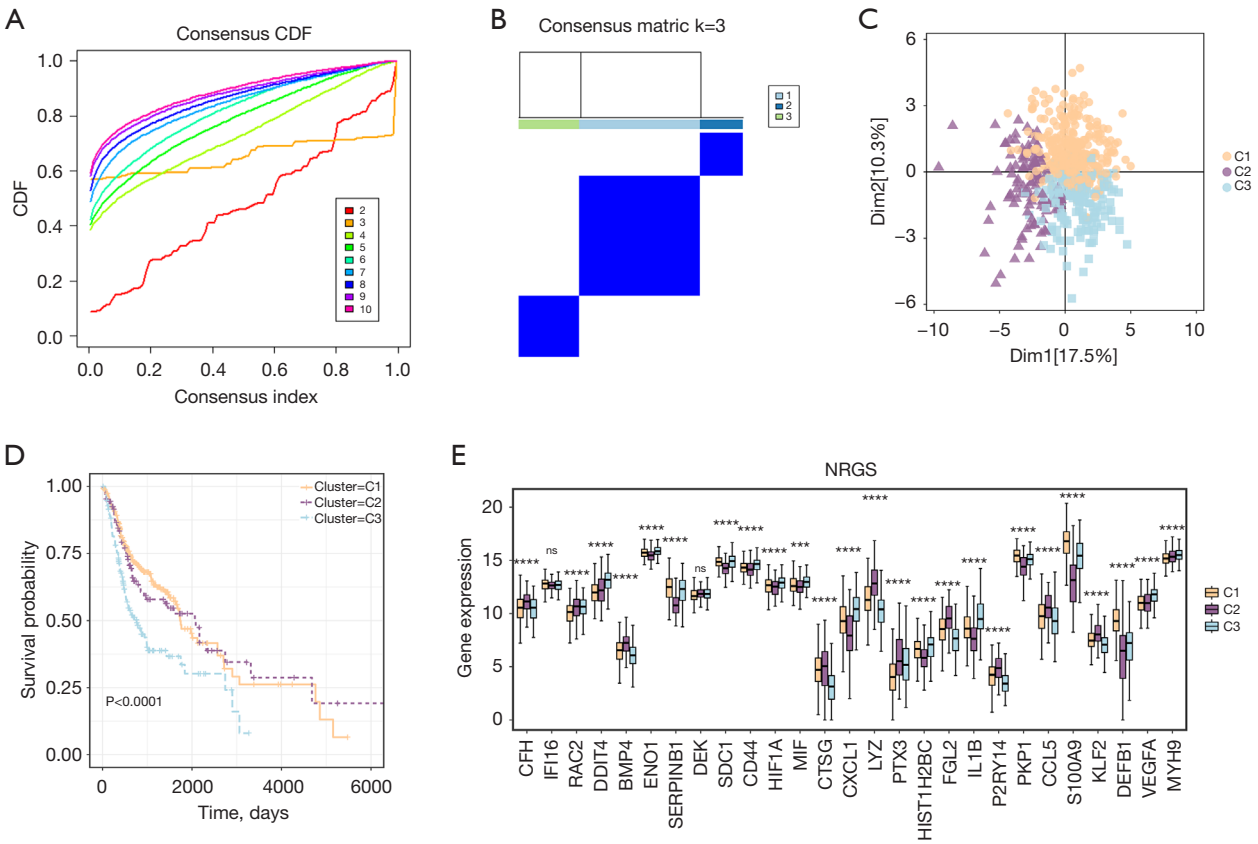

Figure 3 Identification of NET-related molecular subtypes in LSCC. (A,B) CDF and consensus matrix. (C) PCA analysis. (D) Survival probability in different subtypes. (E) Gene expression of DE-NRGs in different subtypes. ***, P<0.001; ****, P<0.0001; ns, no significant. CDF, cumulative distribution function; DE, differentially expressed; LSCC, laryngeal squamous cell carcinoma; NRGs, neutrophil extracellular trap-related genes; NET, neutrophil extracellular trap; PCA, principal components analysis.

varied significantly among the three subtypes (P<0.05, *Figure 4C*). Given the correlation of subtypes with NET, the infiltration of neutrophils among the three subtypes was further investigated using four additional algorithms. The abundance of neutrophils was significantly lower in C2 (P<0.05, *Figure 4D*). To further explore the response to immunotherapy among different subtypes, the expression of immune checkpoint genes programmed death ligand 1 (*PD-L1*) and programmed death 1 (*PD-1*) was compared among the three subtypes. The results showed that these two immune checkpoint genes were significantly higher in C2 (P<0.01, *Figure 4E*).

Construction and evaluation of the prognostic model

A prognostic model was developed using LASSO regression analysis to further elucidate the role of NET in LSCC. Seven hub NRGs were identified, including *ENO1*, *CD44*, *PTX3*, *P2RY14*, *CCL5*, *KLF2*, and *MYH9* (*Figure 5A*). The risk score for each sample was calculated according to the formula: Risk score = 0.178×*ENO1* + 0.005×*CD44* + 0.091×*PTX3* – 0.095×*P2RY14* – 0.015×*CCL5* – 0.007×*KLF2* + 0.047×*MYH9*. All samples were divided into high-risk and low-risk groups based on the median risk score. Accuracy of the prognostic model was evaluated using KM and time-dependent ROC curves. Results showed that the OS was significantly worse in the high-risk group (P<0.0001, *Figure 5B*). The ROC curve showed that the area under curve (AUC) values for 1-, 3-, and 5-year OS were 0.607, 0.681, and 0.626, respectively (*Figure 5B*). Calibration curves and decision curves further confirmed these results (*Figure 5C*,*5D*).

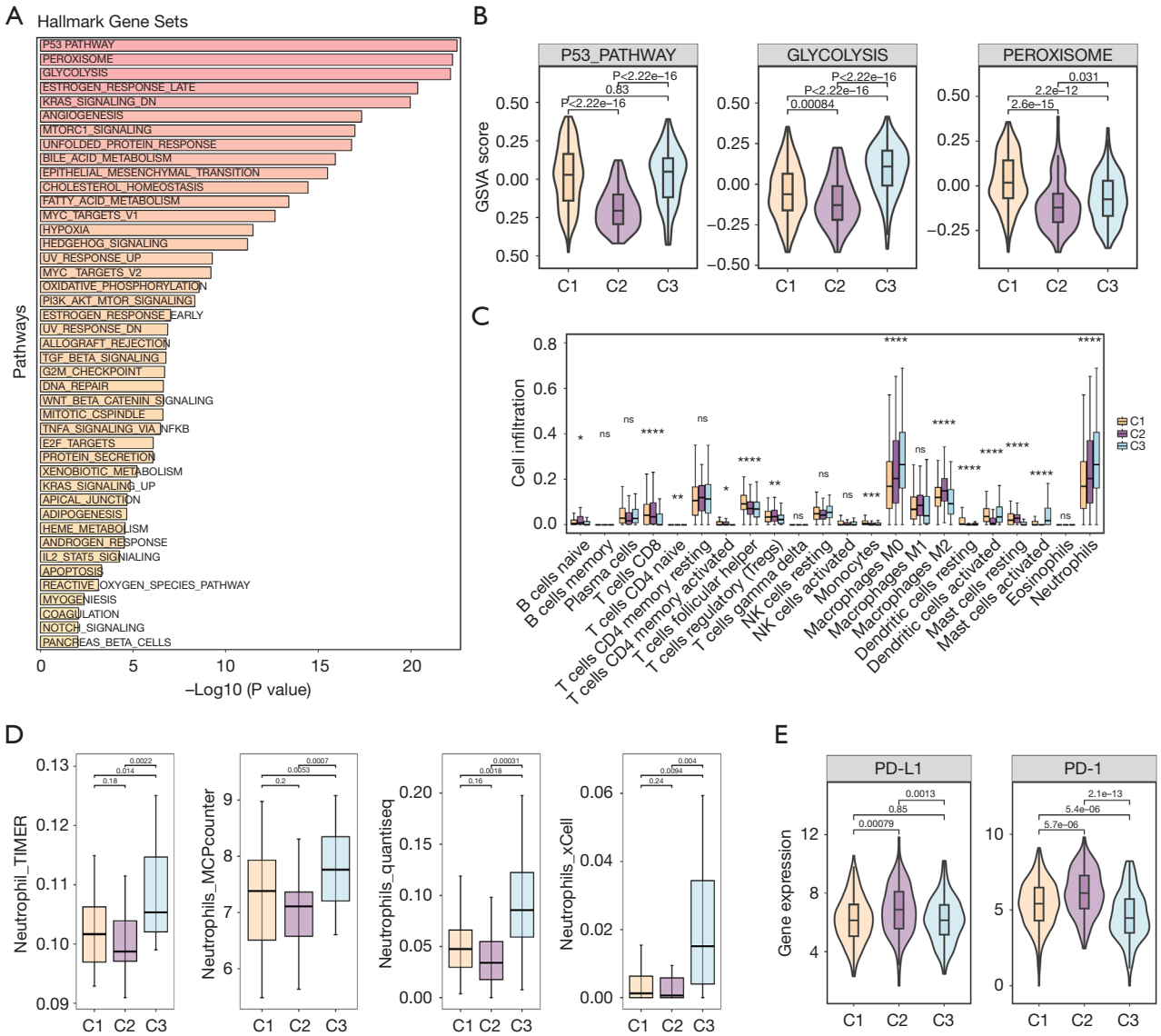

Figure 4 Immune landscape in three subtypes. (A) Pathways associated with NET. (B) GSVA scores among 3 subtypes. (C) Immune cell infiltration analysis using CIBERSORT. *, P<0.05; **, P<0.01; ***, P<0.001; ****, P<0.0001; ns, no significant. (D) Validation of neutrophil abundance using other 4 algorithms among 3 subtypes. (E) Immune check-point gene expression among 3 subtypes. GSVA, gene set variable analysis; NET, neutrophil extracellular trap; PD-L1, programmed death ligand 1; PD-1, programmed death 1; TIMER, Tumor Immune Estimation Resource.

Validation of the prognostic model

Subsequently, the robustness of the prognostic model was further investigated. In both the test set and the external validation set (GSE27020), the OS of the high-risk group was significantly worse than the low-risk group (*Figure 6A,6B*). The ROC curves showed that the AUC values for 1-, 3-, and 5-year OS exceeded 0.61 in both datasets (*Figure 6A,6B*).

Considering that patients' survival prognosis is influenced by factors such as age and tumor grade, we further validated the model's generalizability and robustness by classifying the TCGA-HNSC samples into different groups based on age, tumor grade, alcohol consumption, smoking history, molecular targeted therapy, and radiotherapy. The results showed that the 3-year OS AUC values were above 0.62

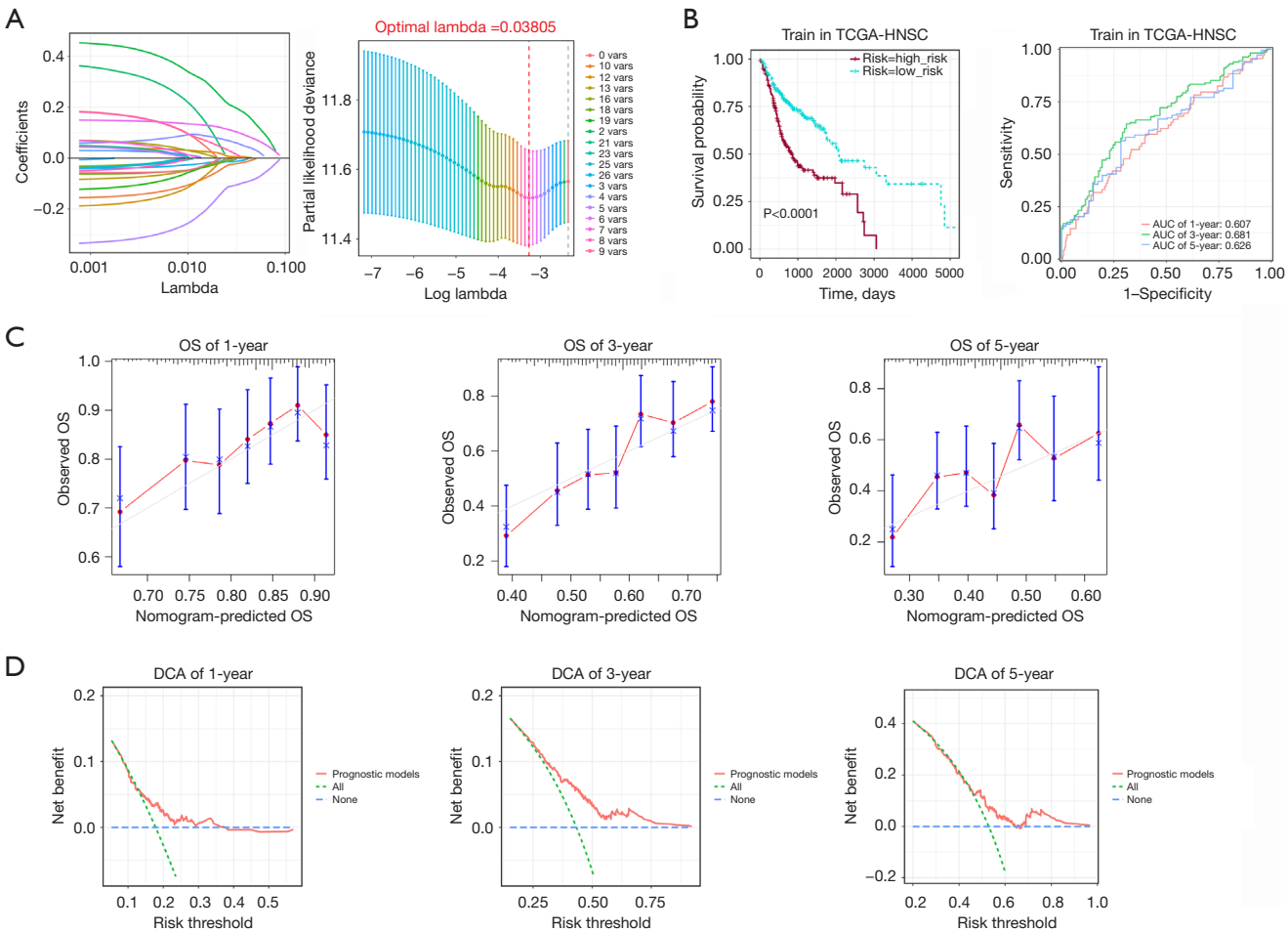

Figure 5 Construction and evaluation of the prognostic model. (A) LASSO regression analysis was performed on 27 DE-NRGs. (B) OS in low-risk and high-risk groups and AUC values of OS at 1-, 3-, and 5-year. (C) Calibration curves of OS at 1-, 3-, and 5-year. (D) Decision curve of OS at 1-, 3-, and 5-year. HNSC, head and neck squamous cell carcinoma; AUC, area under curve; DCA, decision curve analysis; DE, differentially expressed; LASSO, least absolute shrinkage and selection operator; NRGs, neutrophil extracellular trap-related genes; OS, overall survival; TCGA, The Cancer Genome Atlas.

across all stratified levels (*Table 1*).

Prognostic performance of 7 hub NRGs

Furthermore, the predictive performance of hub genes was explored. *ENO1*, *CD44*, *PTX3*, and *MYH9* were harmful factors [hazard ratio (HR) >1], *P2RY14*, *CCL5*, and *KLF2* were protective factors (HR <1, *Figure 7A*). In addition, expression levels of *ENO1*, *CD44*, *PTX3*, and *MYH9* were higher in the high-risk group while expressions of *P2RY14*, *CCL5*, and *KLF2* were lower in the high-risk group (P<0.05, *Figure 7B-7H*).

Discussion

Despite advances in the diagnosis and treatment of LSCC, the proportion of patients with advanced LSCC continues to increase significantly, leading to poor overall prognosis due to its high recurrence rate (15,16). Numerous studies have indicated that neutrophils promote tumor development and progression through the formation of NETs, an emerging hotspot in oncology (17,18). In this study, LSCC was divided into three molecular subtypes based on NRGs, with C3 showing the poorest prognosis. There were significant differences in the TME among these

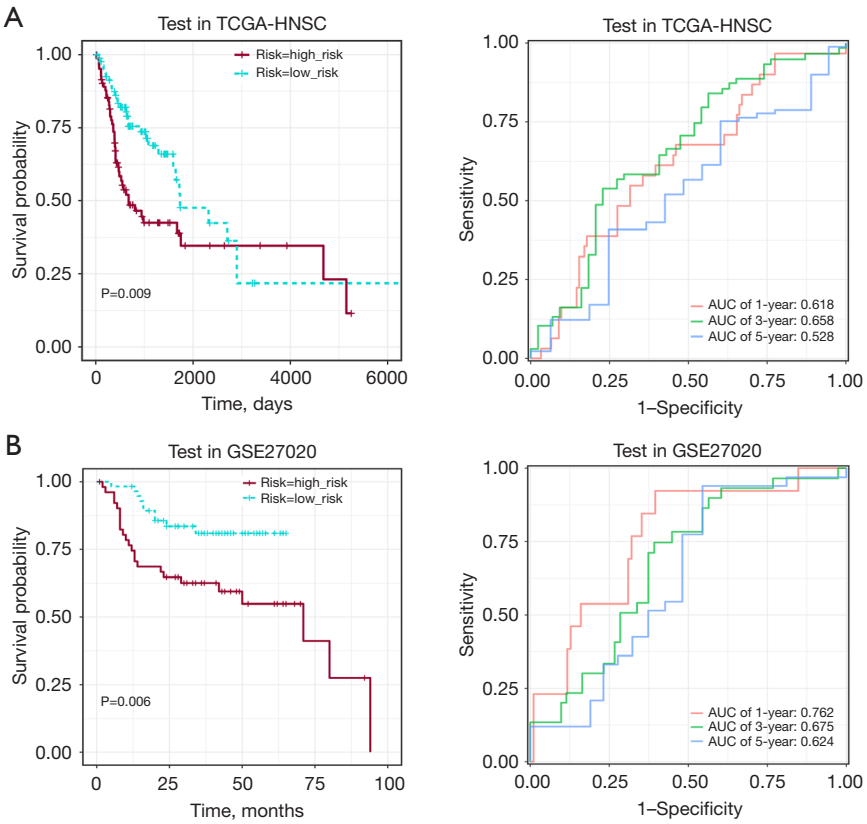

Figure 6 Validation of the prognostic model. (A) OS in low-risk and high-risk groups and AUC values of OS at 1-, 3-, and 5-year in test set. (B) OS in low-risk and high-risk groups and AUC values of OS at 1-, 3-, and 5-year in GSE27020. AUC, area under curve; HNSC, head and neck squamous cell carcinoma; OS, overall survival; TCGA, The Cancer Genome Atlas.

three subtypes. Additionally, we identified seven hub NRGs and constructed a robust prognostic risk model. These seven hub NRGs are potential prognostic markers for LSCC.

Multi-omics studies have shown that HNSC is a highly heterogeneous tumor in an immunosuppressive state (19). NETs may play a crucial role in the TME and are essential for cancer immunotherapy (20). Based on 27 DE-NRGs, this study identified three distinct LSCC molecular subtypes according to the TCGA-HNSC cohort. The prognosis of C1 and C2 was better than that of C3. GSVA identified pathways enriched with NRGs, among which the p53 pathway was highly associated. p53 plays a central role in mediating immune functions by exerting anti-inflammatory effects by inhibiting NF-κB activity (21). Previous studies have shown that p53 enhances the immune response to cancer by upregulating the expression of major histocompatibility complex class I (MHC1) by upregulating endoplasmic reticulum aminopeptidase 1 (ERA1) (22,23). Our study indicated that the GSVA score of the p53 pathway in C2 is significantly lower than in the other two subtypes, suggesting that the p53 pathway may be suppressed in C2.

The TME includes tumor, stromal, and immune cells (24). We conducted immune cell infiltration analysis to investigate the association of three subtypes with immune status further. Significant differences in T cells, B cells, dendritic cells, mast cells, and neutrophils were observed among the three subtypes. These results further confirm that LSCC is an immune-infiltrative tumor (25,26). Among these cells, we focused on neutrophils. Proteins produced by neutrophils are likely to directly or indirectly influence TME remodeling (27). To improve accuracy, we re-evaluated the infiltration abundance of neutrophils in different subtypes using four other algorithms. The results consistently indicated that neutrophil infiltration levels were lowest in C2 and highest in C3. Liu *et al.* proposed that neutrophils enhance the proliferation, migration,

Table 1 Validation of the model's generalizability and robustness

Regroup factors	Group	Sample	Kaplan-Meier P value	AUC (3-year)
Age (years)	<60	249	<0.001	0.716
	≥60	316	<0.001	0.647
Alcohol history	No	182	<0.001	0.644
	Yes	370	<0.001	0.699
	Unknown	13	–	–
Grade	G1-G2	397	<0.001	0.627
	G3-G4	142	<0.001	0.732
	Unknown	26	–	–
Radiotherapy	No	170	<0.001	0.712
	Yes	304	<0.001	0.685
	Unknown	91	–	–
Smoking history (years)	<3	398	<0.001	0.673
	≥3	154	<0.001	0.684
	Unknown	13	–	–
Targeted therapy	No	281	<0.001	0.684
	Yes	150	<0.001	0.73
	Unknown	134	–	–

AUC, area under curve.

and invasion of LSCC (28). Neutrophil density helps predict the prognosis of LSCC patients (29). PD-L1+ neutrophils inhibit T cell proliferation and activation in the LSCC TME, predicting poor prognosis (30). Among the three identified subtypes, C2 showed the highest PD-L1 expression. This aligns with the previous finding that the p53 pathway is suppressed in C2. In lung cancer, loss of p53 activity has been observed to upregulate PD-L1 expression (31). The observations regarding the immune microenvironment partially explain the better prognosis of C2, and our results also suggest that C2 may respond better to immunotherapy.

Additionally, based on these 27 DE-NRGs, we constructed a risk model to predict the prognosis of LSCC patients. The OS of the high-risk group was significantly lower than that of the low-risk group. Consistent results were observed in external datasets, suggesting the robustness of this risk model. Among the seven hub genes (*ENO1*, *CD44*, *PTX3*, *P2RY14*, *CCL5*, *KLF2*, and *MYH9*) constituting the risk model, our study showed that *ENO1*, *CD44*, *PTX3*, and *MYH9* were harmful factors, while the other three genes were protective factors. ENO1 is an enzyme that catalyzes glycolysis. It promotes the migration and invasion of oral squamous cell carcinoma (OSCC) by regulating macrophage IL-6 secretion (32), and it can also impair T cell proliferation in OSCC (33). The expression of CD44 has been identified as a potential marker for more aggressive LSCC (34). PTX3 is involved in the innate immune response and can promote HNSC metastasis by upregulating vimentin signaling (35). MYH9, an important component of the cytoskeleton, acts as a metastatic marker in HNSC and induces epithelial-mesenchymal transition (EMT) in esophageal squamous cell carcinoma to promote cancer cell metastasis (36). P2RY14 is involved in the regulation of the immune system through its role in the stem cell compartment (37). Downregulation of P2RY14 in HNSC is associated with poor prognosis and larger tumors (38). CCL5 is a chemokine that attracts immune cells such as T cells and monocytes to sites of inflammation. CCL5 is associated with OS in OSCC, and inhibition of the CCR5/CCL5 axis can suppress OSCC metastasis (39). KLF2 is a tumor suppressor gene that is downregulated

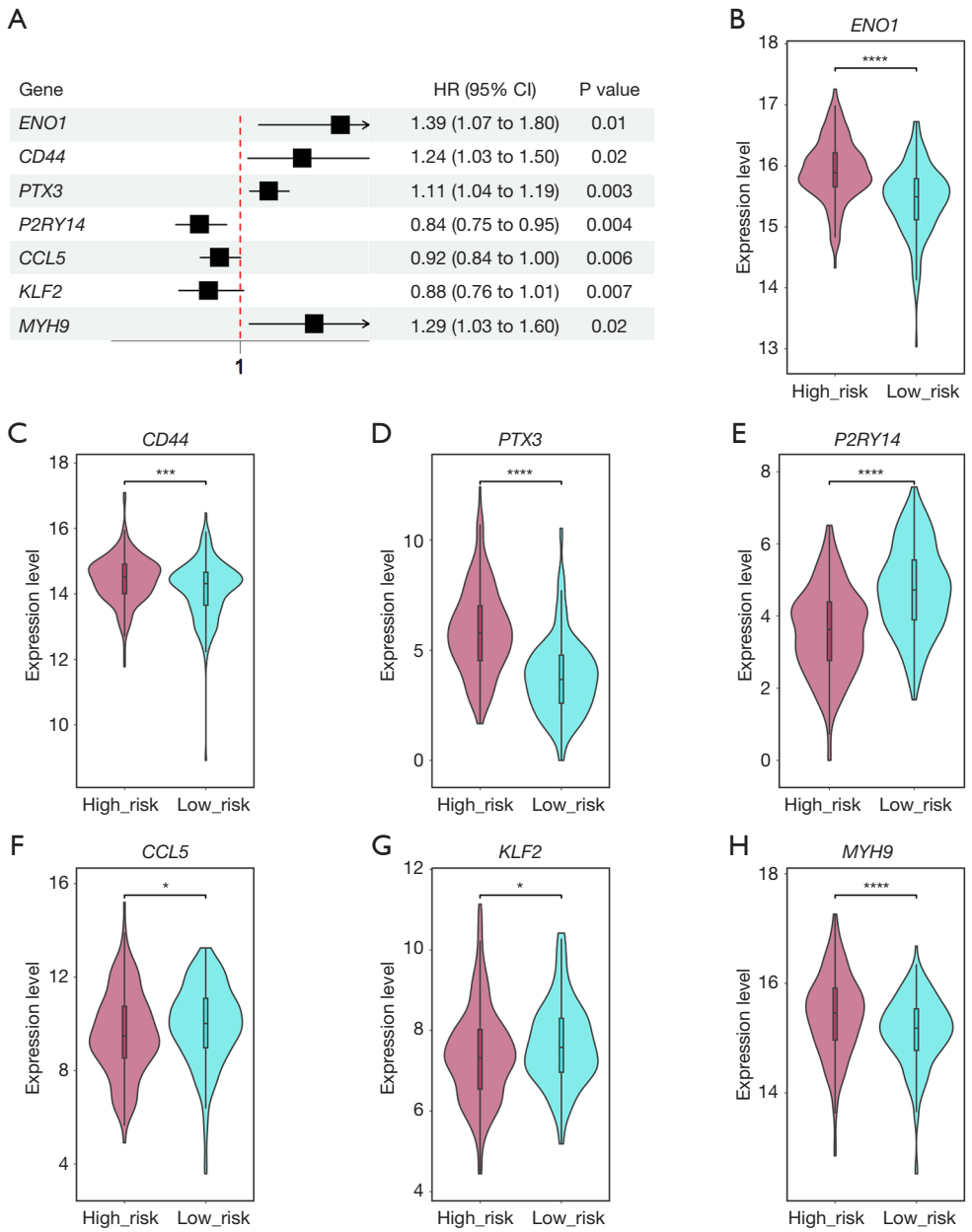

Figure 7 Prognostic performance of 7 hub NRGs. (A) Forest plot of 7 hub genes. (B-H) Expression levels of *ENO1*, *CD44*, *PTX3*, *P2RY14*, *CCL5*, *KLF2*, and *MYH9*. *, P<0.05; ***, P<0.001; ****, P<0.0001. HR, hazard ratio; CI, confidence interval; NRGs, neutrophil extracellular trap-related genes.

in OSCC cells and tissues (40). These studies suggest the potential roles of the seven hub genes in LSCC. In our study, *ENO1*, *CD44*, *PTX3*, and *MYH9* were significantly upregulated in the high-risk group, while the other three genes were downregulated. However, their specific roles in LSCC require further investigation.

There are several limitations in this study. First, the analysis was based on common databases, which may introduce selection bias. Second, while the model was validated in external datasets, prospective clinical validation is necessary to confirm its utility in clinical practice. Third, the molecular mechanisms by which NETs and their related genes influence LSCC progression and response to therapy require further experimental validation.

Conclusions

In conclusion, this study comprehensively analyzed NRGs in LSCC, identifying 3 different molecular subtypes and constructing a robust prognostic model. These findings enhance our understanding of LSCC biology and offer potential biomarkers for risk stratification and personalized treatment, paving the way for improved clinical management of LSCC patients.

Acknowledgments

None.

Footnote

Reporting Checklist: The authors have completed the TRIPOD reporting checklist. Available at https://tcr.amegroups.com/article/view/10.21037/tcr-24-1531/rc

Peer Review File: Available at https://tcr.amegroups.com/article/view/10.21037/tcr-24-1531/prf

Funding: None.

Conflicts of Interest: All authors have completed the ICMJE uniform disclosure form (available at https://tcr.amegroups.com/article/view/10.21037/tcr-24-1531/coif). The authors have no conflicts of interest to declare.

Ethical Statement: The authors are accountable for all aspects of the work in ensuring that questions related to the accuracy or integrity of any part of the work are appropriately investigated and resolved. The study was conducted in accordance with the Declaration of Helsinki (as revised in 2013). The Ethics Committee of The First Affiliated Hospital of Gannan Medical University deemed that this research is based on open-source data, so the need for ethics approval was waived.

References

1. Ezeh UC, Al-Awady A, Buitron I, et al. Investigating Disparities in Hypopharyngeal/Laryngeal Cancer Survival in Florida With Geospatial Mapping Analysis. Cancer Control 2024;31:10732748241246958.
2. Zhu X, Heng Y, Ma J, et al. Prolonged Survival of Neutrophils Induced by Tumor-Derived G-CSF/GM-CSF Promotes Immunosuppression and Progression in Laryngeal Squamous Cell Carcinoma. Adv Sci (Weinh) 2024;11:e2400836.
3. Wang W, Wang W, Zhang D, et al. Creation of a machine learning-based prognostic prediction model for various subtypes of laryngeal cancer. Sci Rep 2024;14:6484.
4. Falco M, Tammaro C, Cossu AM, et al. Identification and bioinformatic characterization of a serum miRNA signature for early detection of laryngeal squamous cell carcinoma. J Transl Med 2024;22:647.
5. Li H, Bo S, Guo Y, et al. Identification of hub genes and key modules in laryngeal squamous cell carcinoma. Transl Cancer Res 2024;13:3771-82.
6. Shafqat A, Khan JA, Alkachem AY, et al. How Neutrophils Shape the Immune Response: Reassessing Their Multifaceted Role in Health and Disease. Int J Mol Sci 2023;24:17583.
7. Yang S, Jia J, Wang F, et al. Targeting neutrophils: Mechanism and advances in cancer therapy. Clin Transl Med 2024;14:e1599.
8. Malamud M, Whitehead L, McIntosh A, et al. Recognition and control of neutrophil extracellular trap formation by MICL. Nature 2024;633:442-50.
9. Cristinziano L, Modestino L, Antonelli A, et al. Neutrophil extracellular traps in cancer. Semin Cancer Biol 2022;79:91-104.
10. Zhong W, Wang Q, Shen X, et al. Neutrophil Extracellular Trap is Surrogate Biomarker for Prognosis and Response to Neoadjuvant Therapy in Locally Advanced Rectal Cancer. J Inflamm Res 2023;16:6443-55.
11. Wang Q, Huang Y, Zhu Y, et al. The m6A methyltransferase METTL5 promotes neutrophil extracellular trap network release to regulate hepatocellular carcinoma progression. Cancer Med 2024;13:e7165.
12. Yu Y, Zhang C, Dong B, et al. Neutrophil extracellular traps promote immune escape in hepatocellular carcinoma by up-regulating CD73 through Notch2. Cancer Lett 2024;598:217098.

13. Jiang ZZ, Peng ZP, Liu XC, et al. Neutrophil extracellular traps induce tumor metastasis through dual effects on cancer and endothelial cells. Oncoimmunology 2022;11:2052418.
14. Zhang Y, Guo L, Dai Q, et al. A signature for pan-cancer prognosis based on neutrophil extracellular traps. J Immunother Cancer 2022;10:e004210.
15. Luo L, Liu H. High-grade tumor budding is a risk factor for survival in patients with laryngeal squamous cell carcinoma. Braz J Otorhinolaryngol 2023;89:101310.
16. Zamani R, Rezaei N. Immune-scoring in head and neck squamous cell carcinoma: a scoping review. Expert Rev Clin Immunol 2024;20:1009-17.
17. Ma Y, Wei J, He W, et al. Neutrophil extracellular traps in cancer. MedComm (2020) 2024;5:e647.
18. Zhai R, Gong Z, Wang M, et al. Neutrophil extracellular traps promote invasion and metastasis via NLRP3-mediated oral squamous cell carcinoma pyroptosis inhibition. Cell Death Discov 2024;10:214.
19. Sun Y, Chen S, Lu Y, et al. Single-cell transcriptomic analyses of tumor microenvironment and molecular reprograming landscape of metastatic laryngeal squamous cell carcinoma. Commun Biol 2024;7:63.
20. Li Q, Chen W, Li Q, et al. A novel neutrophil extracellular trap signature to predict prognosis and immunotherapy response in head and neck squamous cell carcinoma. Front Immunol 2022;13:1019967.
21. Siddiqui SS, Rahman S, Rupasinghe HPV, et al. Dietary Flavonoids in p53-Mediated Immune Dysfunctions Linking to Cancer Prevention. Biomedicines 2020;8:286.
22. Wang B, Niu D, Lai L, et al. p53 increases MHC class I expression by upregulating the endoplasmic reticulum aminopeptidase ERAP1. Nat Commun 2013;4:2359.
23. Chauhan S, Jaiswal S, Jakhmola V, et al. Potential role of p53 deregulation in modulating immune responses in human malignancies: A paradigm to develop immunotherapy. Cancer Lett 2024;588:216766.
24. Su K, Zhou Z, Yi Q, et al. Systemic Analysis on the Features of Immune Microenvironment Related to Prognostic Signature in Head and Neck Squamous Cell Carcinoma. Front Genet 2022;13:860712.
25. Arcovito G, Palomba A, Gallo O, et al. The Histological Background of Recurrence in Laryngeal Squamous Cell Carcinoma: An Insight into the Modifications of Tumor Microenvironment. Cancers (Basel) 2023;15:3259.
26. Rodrigo JP, Sánchez-Canteli M, López F, et al. Tumor-Infiltrating Lymphocytes in the Tumor Microenvironment of Laryngeal Squamous Cell Carcinoma: Systematic Review and Meta-Analysis. Biomedicines 2021;9:486.
27. Garley M. Unobvious Neutrophil Extracellular Traps Signification in the Course of Oral Squamous Cell Carcinoma: Current Understanding and Future Perspectives. Cancer Control 2023;30:10732748231159313.
28. Liu T, Zong S, Jiang Y, et al. Neutrophils Promote Larynx Squamous Cell Carcinoma Progression via Activating the IL-17/JAK/STAT3 Pathway. J Immunol Res 2021;2021:8078646.
29. Zhang D, Tang D, Heng Y, et al. Prognostic Impact of Tumor-Infiltrating Lymphocytes in Laryngeal Squamous Cell Carcinoma Patients. Laryngoscope 2021;131:E1249-55.
30. Tang D, Zhang D, Heng Y, et al. Tumor-Infiltrating PD-L1+ Neutrophils Induced by GM-CSF Suppress T Cell Function in Laryngeal Squamous Cell Carcinoma and Predict Unfavorable Prognosis. J Inflamm Res 2022;15:1079-97.
31. Chamoto K, Hatae R, Honjo T. Current issues and perspectives in PD-1 blockade cancer immunotherapy. Int J Clin Oncol 2020;25:790-800.
32. Lin Y, Zhang W, Liu L, et al. ENO1 Promotes OSCC Migration and Invasion by Orchestrating IL-6 Secretion from Macrophages via a Positive Feedback Loop. Int J Mol Sci 2023;24:737.
33. Wang J, Man Q, Zhong N, et al. ENO1 Binds to ApoC3 and Impairs the Proliferation of T Cells via IL-8/STAT3 Pathway in OSCC. Int J Mol Sci 2022;23:12777.
34. Puzzo L, Bianco MR, Salvatorelli L, et al. CD44, PDL1, and ATG7 Expression in Laryngeal Squamous Cell Carcinomas with Tissue Microarray (TMA) Technique: Evaluation of the Potential Prognostic and Predictive Roles. Cancers (Basel) 2023;15:2461.
35. Chan SH, Tsai JP, Shen CJ, et al. Oleate-induced PTX3 promotes head and neck squamous cell carcinoma metastasis through the up-regulation of vimentin. Oncotarget 2017;8:41364-78.
36. Yang B, Liu H, Bi Y, et al. MYH9 promotes cell metastasis via inducing Angiogenesis and Epithelial Mesenchymal Transition in Esophageal Squamous Cell Carcinoma. Int J Med Sci 2020;17:2013-23.
37. Meng L, He X, Hong Q, et al. CCR4, CCR8, and P2RY14 as Prognostic Factors in Head and Neck Squamous Cell Carcinoma Are Involved in the Remodeling of the Tumor Microenvironment. Front Oncol 2021;11:618187.
38. Li Q, Xu L, Li Y, et al. P2RY14 Is a Potential Biomarker of Tumor Microenvironment Immunomodulation and

Favorable Prognosis in Patients With Head and Neck Cancer. Front Genet 2021;12:670746.
39. González-Arriagada WA, Coletta RD, Lozano-Burgos C, et al. CR5/CCL5 axis is linked to a poor outcome, and inhibition reduces metastasis in oral squamous cell carcinoma. J Cancer Res Clin Oncol 2023;149:17335-46.
40. Kou Y, Zhang Y, Rong X, et al. Simvastatin inhibits proliferation and promotes apoptosis of oral squamous cell carcinoma through KLF2 signal. J Oral Biosci 2023;65:347-55.

Cite this article as: Wu G, Jin R, Liao J, Zhang J, Liu X. Molecular subtype and prognostic model of laryngeal squamous cell carcinoma based on neutrophil extracellular trap-related genes. Transl Cancer Res 2025;14(3):1772-1785. doi: 10.21037/tcr-24-1531